

# A comprehensive 3D model for rock slopes based on micromechanics

Peter A Cundall  
Itasca Consulting Group, Inc.

Branko Damjanac  
Itasca Consulting Group, Inc.

## Abstract

*Conventional design methods for rock slopes involve the use of continuum strength criteria (such as Hoek Brown) for the rock mass, in which yield of both intact material and discontinuities (joints) must occur for overall failure to take place. Empirical methods often are used to estimate parameters for the rock mass because of the impossibility of testing directly (to failure) a large extent of rock. Alternatively, a numerical approach, called the synthetic rock mass (SRM), has been developed, based on the distinct element method. Rather than using finite-sized particles, greater efficiency can be realized with a "lattice" of point masses connected by springs. This model allows fracture, by breakage of springs, and joint slip, using a smooth representation of joint segments. The methodology of a new 3D lattice program, Slope Model, is described, which accepts a general DFN (discrete fracture network). Fluid flow throughout the jointing network also is modeled, with the resulting pressures being used to compute effective stresses on each joint element. Pressure changes also arise through mechanical coupling. Examples are presented of the use of Slope Model to determine the stability, flow regime and transient coupled response of 3D jointed rock slopes due to mining activities.*

## INTRODUCTION

Conventional design methods for rock slopes involve the use of continuum strength criteria (such as Hoek Brown) for the rock mass. The term "rock mass" denotes a large volume of fractured rock in which yield of both intact material and discontinuities (joints) must occur for overall failure to take place. The difficulty in characterizing a rock mass arises from the impossibility of testing directly (to failure) a large extent of rock. Thus, empirical methods often are used to estimate the parameters for the rock-mass strength criterion. Such approaches ignore many important aspects, such as size effect and the complex way in which localized failure may propagate in a jointed medium (e.g., by the fracture of rock bridges).

Recently, a numerical approach, called the synthetic rock mass (SRM) and described by Pierce et al. (1), has been developed, based on the distinct element method. The SRM usually is realized as a bonded-particle assembly representing brittle rock containing multiple joints, each one consisting of a planar array of bonds that obey a special model, the smooth joint model (SJM). The SJM allows slip and separation at particle contacts, while respecting the given joint orientation rather than local contact orientations. Overall failure of a synthetic rock mass depends on both fracture of intact material (bond breaks) as well as yield of joint segments. The modeling of intact-rock fracture by bonded-particle models is described by Potyondy and Cundall (2). Note that rock-mass behavior is an emergent property of the SRM model, in contrast to behavior that must be imported as constitutive laws — as in finite element models, for example.

Previous SRM models have used the general-purpose codes PFC2D (3) and PFC3D (4), which employ assemblies of circular particles bonded together. Much greater efficiency can be realized for brittle rock if a "lattice," consisting of point masses (nodes) connected by springs, replaces the balls and contacts (respectively) of PFC3D. The lattice model still allows fracture, by breakage of springs, and joint slip, using a modified version of the SJM (smooth joint model). The new 3D program, Slope Model, described here, is based on such a lattice representation of brittle rock.

## FORMULATION AND APPLICABILITY OF SLOPE MODEL

The numerical formulation of the code is provided in the Appendix. It is a fully dynamic solution, with damping used to converge to steady-state solutions. As with other Itasca codes, the dynamic formulation allows the code to follow highly nonlinear behavior without numerical difficulty. In the case of Slope Model, the nonlinear behavior consists of rock fracture and joint slip/opening. The program accepts a general DFN (discrete fracture network) consisting of multiple joint segments that are overlaid on the lattice springs. Springs that are part of a joint segment obey a joint constitutive law, which is applied in the normal and shear joint directions rather than the local lattice spring direction. Fluid flow throughout the joint system also is modeled by means of a network of parallel-plate reservoirs connected by pipes. The reservoir pressures are used to compute effective stresses (and, hence, failure conditions) on each joint element. Other aspects of fluid/mechanical coupling also are included — the influence of local stress or separation on aperture (and, hence, permeability) and the direct influence of deformation on fluid pressure. Thus, Slope Model can simulate the time-evolution of the field of pressures and flows due to mining activities (such as bench removal) and the resulting influence on stability.

The main application for Slope Model is the assessment of stability of large slopes in jointed rock masses, with fully-coupled fluid interaction. Although other codes, such as 3DEC (5), can simulate 3D stability of blocky systems with fluid interaction, Slope Model has the added capability to allow new fracturing through intact rock. This feature is important for high slopes, in which the induced stresses may be sufficient to cause significant new fracturing. Although the code has been demonstrated only on small test cases to date, it should be able to solve large models with millions of lattice nodes and thousands of disc-shaped joints. Slope Model is compiled as a multi-threaded, 64-bit code for Windows operating systems, so there is no limit to model size, apart from the RAM available.

## EXAMPLES AND VALIDATIONS

Slope Model has so many aspects that it is only possible to provide here a small sampling of the mechanical, fluid and coupled behavior that may be simulated by the code. In particular, a number of validations have been performed but not reproduced here, such as comparisons of the transient fluid response compared to analytical solutions.

### Wedge Failure Validation

A well-documented form of failure in jointed-rock slopes is 3D wedge failure. For example, Hoek and Bray (6) provide stability charts that enable the factor of safety of single wedges to be determined under a range of different conditions. The simulation of wedge failure represents a good test of Slope Model because the code does not use continuous joint planes, as used in more conventional codes, such as 3DEC. Rather, a joint “plane” consists of those springs that are intersected by the track of the plane. Each such spring obeys the SJM. Thus, the sliding block actually is represented as a network of nodes and springs bounded by sets of SJM springs. Although this network has far more degrees-of-freedom than a rigid sliding-block, it should act as if it were a single element as far as the determination of factor of safety is concerned.

A 75°, 110-m high slope is simulated with Slope Model. The slope contains two joints that form a wedge that is symmetrical about the slope face. For the case of two joints with dips of 40°, dip directions of 45° and 135°, and a friction coefficient of 0.5 (friction angle of 26.57°), the system is unstable — see Figure 1, which shows actively moving nodes in red. To confirm instability, the velocity history monitored at the centre of the slope crest is observed to increase continuously. In contrast, a simulation with dip directions of 40° and 140° exhibits a stable final state, in which the velocity converges to zero.

#### SLOPE MODEL 1.00

©2009 Itasca Consulting Group, Inc.

Step 4309  
6/16/2009 5:49:54 PM

#### Sketch Model

##### Elements

- Rock
- Seams
- y-vel. history
- z-vel. history
- fluid pressure history
- fluid flow rate history
- Excavation
- origin

#### Velocity Field

Maximum: 6.90011

Scale: 0.43844

- 0.0000E+00
- 2.0000E-03
- 4.0000E-03
- 6.0000E-03
- 8.0000E-03
- 1.0000E-02
- 1.2000E-02
- 1.4000E-02
- 1.6000E-02
- 1.8000E-02
- 2.0000E-02

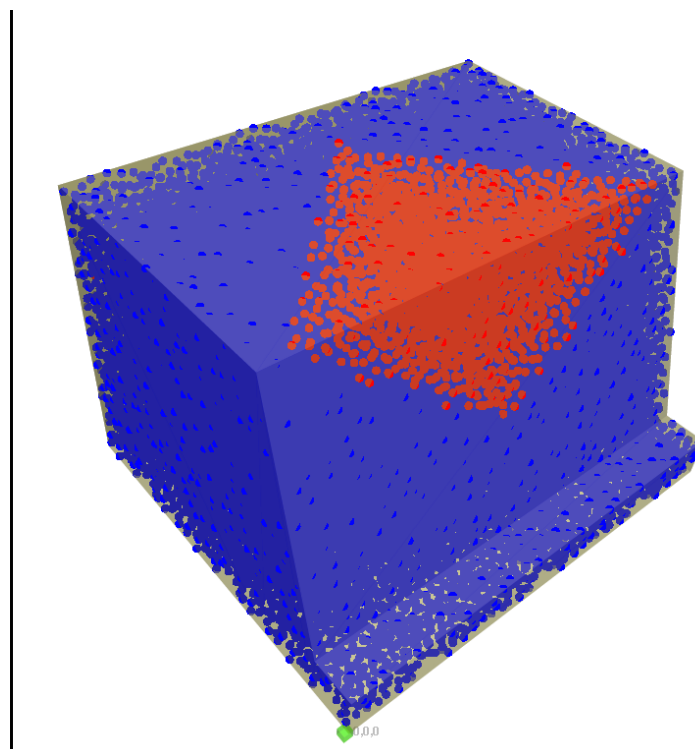


**Figure 1** – Failing wedge, red nodes have elevated velocity [The two bounding joints in this example have dips of 40° and dip directions of 45° and 135°. (Note that the strike of the slope is North.)]

In order to obtain an estimate of conditions that correspond to a factor of safety of 1.0, several simulations were performed in which dip directions were varied. A bracketing method was used whereby the interval between neighboring stable and unstable states was halved progressively until the interval was reduced to around  $\pm 0.5\%$ . Accordingly, the results shown in Table 1 were obtained. The results are superimposed on the plot from Hoek and Bray (6), shown in Figure 2: there is good agreement between the analytic solutions and the solutions using Slope Model. Note that the formula for factor of safety is  $F=2A \tan \phi$  when the friction angle,  $\phi$ , for both planes is equal. In the cases reported here,  $\tan \phi=0.5$ , so  $F=A$ , where A comprises the vertical axes of Figure 2.

Dip (°)	Difference in dip direction (of the two planes) in degrees, for factor of safety of 1.0, found from <i>Slope Model</i> simulations
30	54.4
40	94.4
50	113.4

**Table 1** – *Slope Model* results in terms of dip-direction differences necessary for a safety factor of 1.0, for a joint friction coefficient of 0.5.

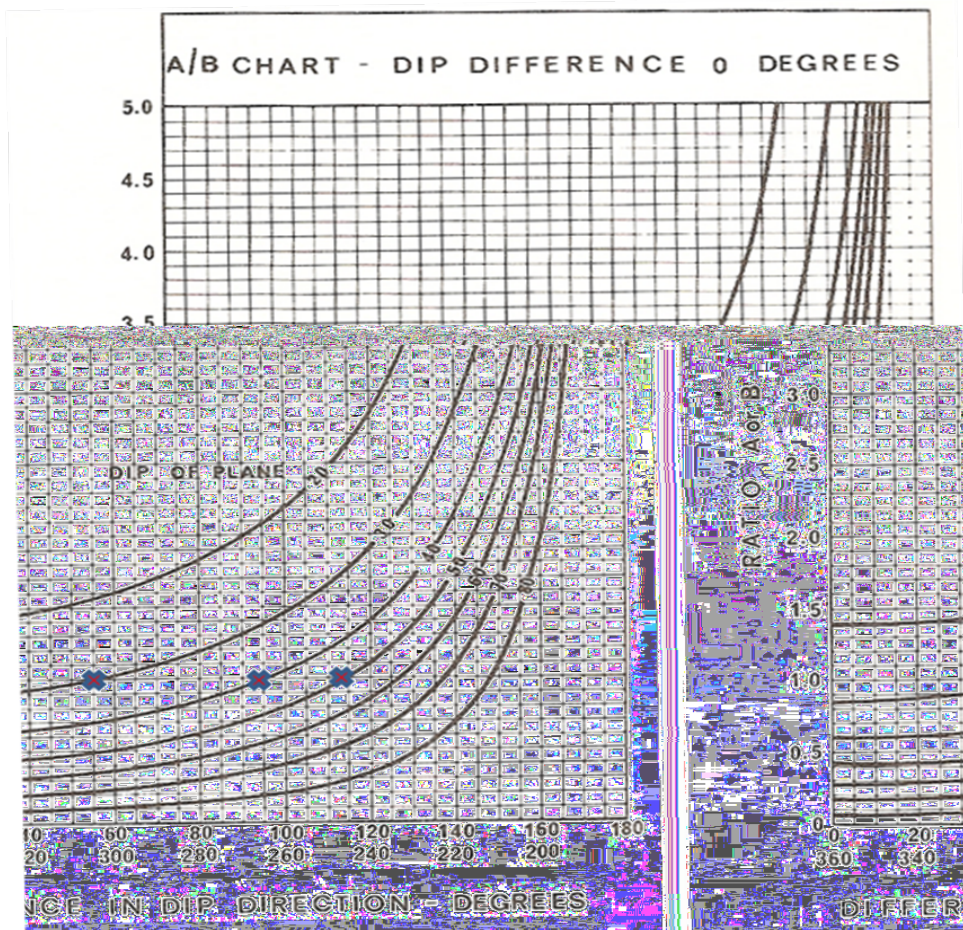


**Figure 2** – Stability chart from Hoek and Bray (6), with points (crosses) superimposed for *Slope Model* simulation results for wedges with plane dips of 30°, 40° and 50° [The vertical axis corresponds to safety factor (see text) for the case where both planes have the same dips. The crosses correspond to simulation results for  $F=A=1$ , for the three dip values.]

### Example of Bridging Fracture

Most joint planes in a rock mass are discontinuous and partly unconnected. Thus, deep-seated failure of a large slope requires fracture through “bridges” of intact rock. As an example of this behavior, Figure 3 shows a 500-m length of a 1000-m high slope consisting of ten benches. There are two discontinuous joint sets, nominally dipping at 30° and 70°, with low values of friction angle. A deep-seated failure is not possible simply by slip on the joint segments, but a simulation with *Slope Model* shows that fractures form in the gaps between the joints so as to allow overall slope failure. This effect can be seen in Figure 4, which shows a cross-sectional slice of the upper part through the center of the slope. Fractures are visible as black dots, with each dot representing a broken spring. The example is simply to demonstrate that *Slope Model* is able to simulate rock bridging with new fractures; the properties are not supposed to be realistic or representative of any particular rock, and, therefore, are not provided.

## SLOPE MODEL 1.00

©2009 Itasca Consulting Group, Inc.

Step 0

7/15/2009 2:28:49 PM

### Sketch Model

#### Elements

- Rock
- Seams
- y-vel. history
- z-vel. history
- fluid pressure history
- fluid flow rate history
- Excavation
- origin

### Joint Trace

- Joint Trace
- Joint 1
- Joint 0

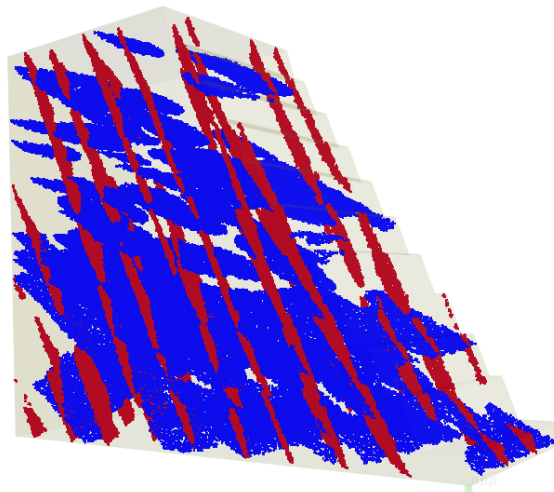


**Figure 3** – 500-m sector of 1000-m high slope with 10 benches showing two discontinuous joint sets

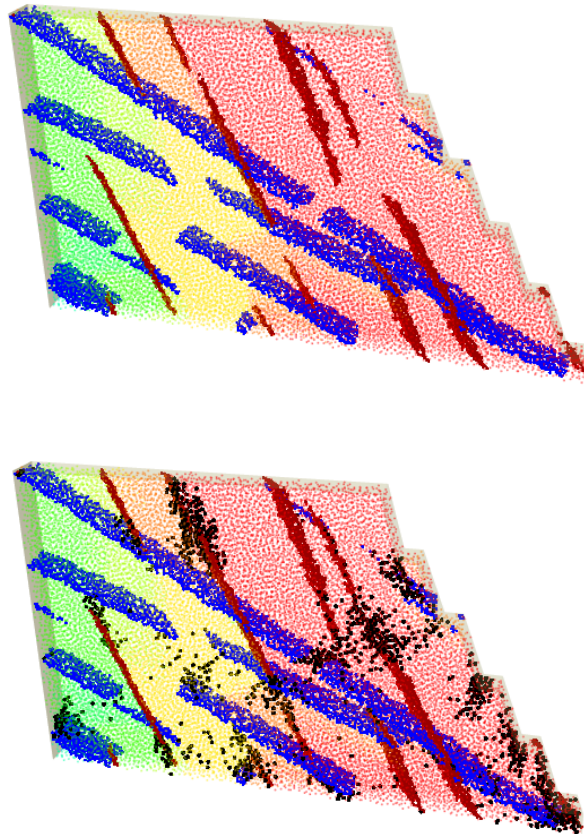


**Figure 4** – Cross-sectional slice through the upper part of the 1000-m slope [Upper view shows the joint traces within the slice; in the lower view, micro-cracks are added. Note that fractures tend to bridge across gaps in the joints, in order to allow deep-seated failure. The background colors denote movement magnitude (red = high).]

### Steady-State, Free-Surface Flow through a Fracture Network

Steady-state fluid flow with free surfaces through a network of fractures is simulated using Slope Model, and the results are compared with a solution obtained using the flow-only code 3FLO (7). Capillary pressures are assumed to be zero in Slope Model; consequently, there is no capillary fringe above the free (phreatic) surface. Therefore, Van Genuchten parameters in the 3FLO model are selected ( $\alpha = 1$ ,  $n = 6$ ) to result in relatively small capillary rise above the free surface. The geometry of the analyzed problem is illustrated in Figure 5. The slope has three benches, each 10-m high and 10-m wide. The slope length is 10 m, striking to the north.

The model includes 15 circular discontinuities, each with hydraulic aperture of  $3 \times 10^{-6}$  m, and target radii ranging from 4 to 12 m (mean of 8 m). In addition there is one persistent vertical joint through the model center. The water levels on the west and east sides of the model are 20 m and 10 m above the model base, respectively. Slope Model is run, by simulating flow only, to steady state for the specified fluid boundary conditions of the model. The results, in terms of joint flow rates and location of phreatic surfaces, are shown in Figure 6. The comparable results, obtained using the code 3FLO, are shown in Figure 7, in which the position of the free water surface is indicated by black crosses. The agreement between the results of the two models is good. Note that 3FLO has been in use for many years and that its formulation is quite different from that of Slope Model. Thus, the example is believed to represent a validation of Slope Model's ability to simulate free-surface flow in a complex jointing network.

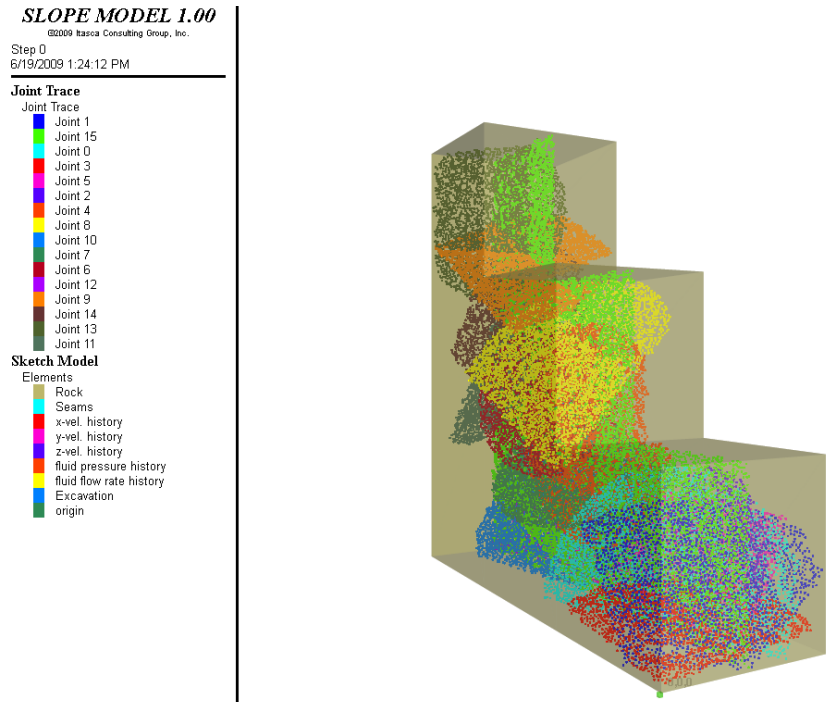


**Figure 5** – Joint traces for flow-only example of Slope Model, containing 16 discontinuities, of which 15 are nominally circular (but truncated by the model boundaries) and one is a persistent vertical joint through the center of the model.

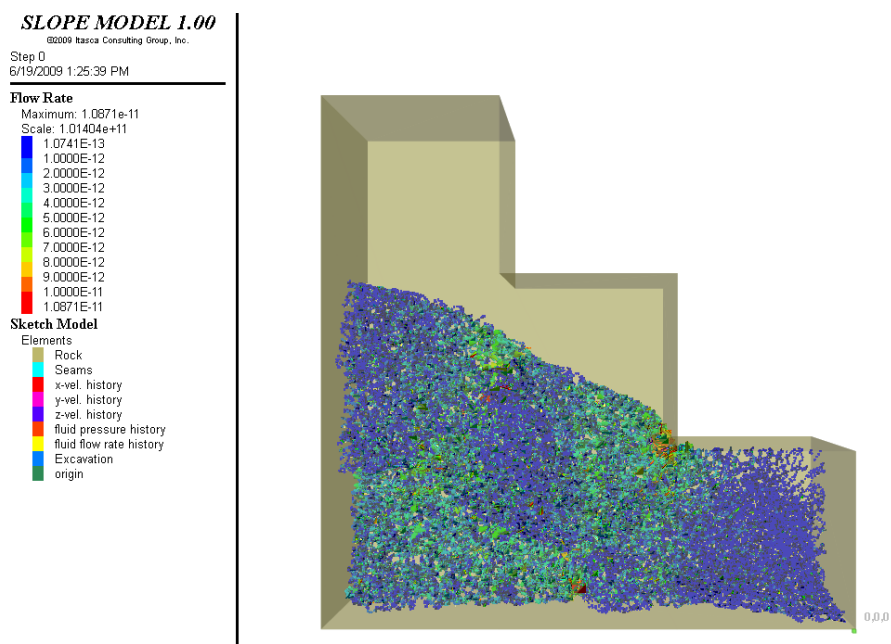


**Figure 6** – Steady-state flow-rate vectors and free-surface location for Slope Model simulation

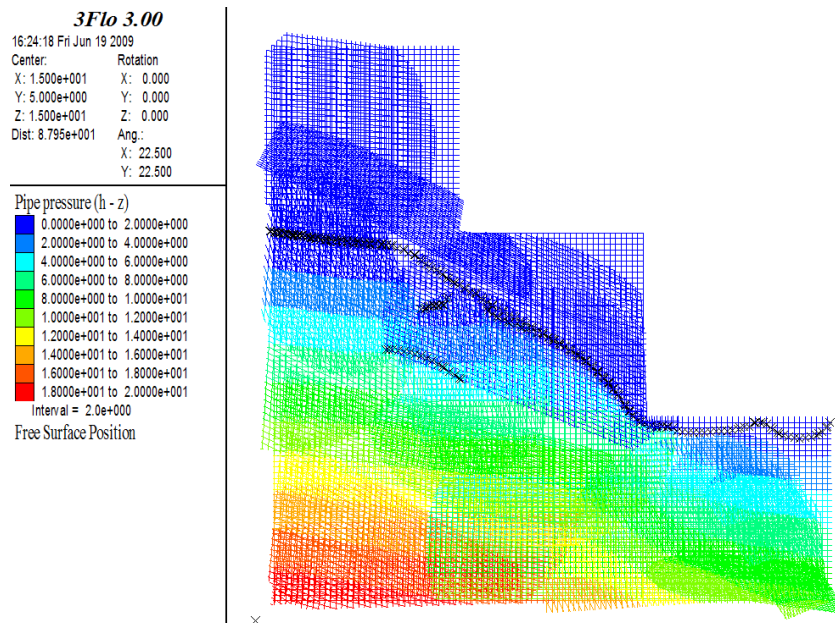


**Figure 7** – Pressure distribution and free-surface locations (black crosses) for 3FLO simulation

### Validation of Effective Stress Formulation

The effective stress calculation in Slope Model is validated by simulating a problem of stability of a block resting under gravity on a fluid-filled joint inclined at an angle  $\alpha$ . The problem as set up with Slope Model is illustrated in Figure 8, which shows the angled joint in blue. Although two joints are included, the fluid pressure is initialized in the inclined joint only. The purpose of the vertical (green) joint is to detach the upper block from the far-field boundary and allow sliding along the inclined joint. If fluid pressures at each point in the angled joint are proportional to the height of the block above the point, the critical friction angle,  $\phi$ , in the joint can be expressed by the following relation:

$$\tan \phi = \frac{\sin \alpha \cos \alpha}{\cos^2 \alpha - \frac{\rho_w}{\rho_r}} \quad (1)$$

where  $\rho_w$  and  $\rho_r$  are densities of water and rock, respectively. Clearly, for a dry joint, Equation (1) degenerates to  $\phi = \alpha$ .

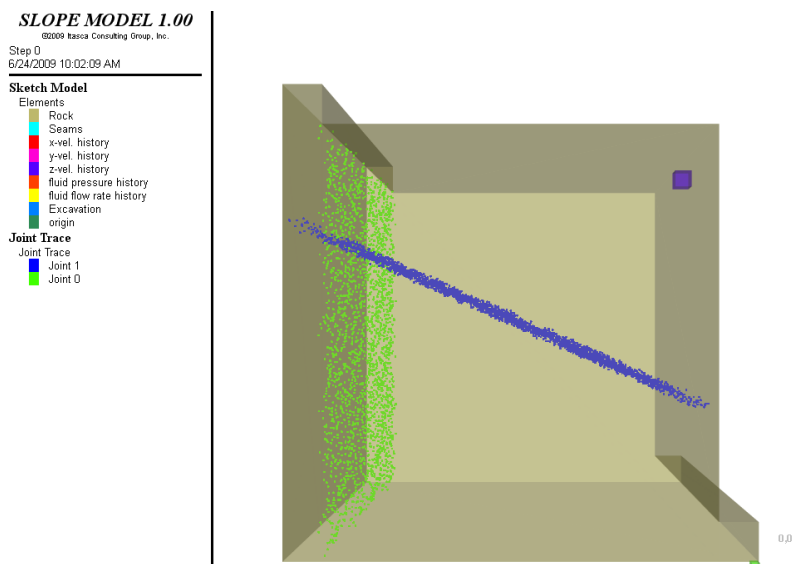


**Figure 8** – Geometry used in validation of effective stress formulation [Fluid flow is introduced into the blue joint; the green joint is included in order to allow the upper block to detach if sliding on the inclined joint occurs.]

In the conducted simulations,  $\rho_w = 1000 \text{ kg/m}^3$ , and  $\rho_r = 2650 \text{ kg/m}^3$ . For the assumed friction coefficient,  $\tan \phi = 0,75$ , the relation in Equation indicates that the critical inclination of the slope is  $\alpha = 22,7^\circ$ . The problem is simulated using Slope Model for the joint inclinations of  $22^\circ$  and  $24^\circ$ . The model for  $22^\circ$  joint inclination should be stable, while  $24^\circ$  joint inclination should result in sliding of the block above the joint.

For 22° joint inclination, the velocity history (monitored at the location of the blue cube in Figure 8) converges to zero, indicating that the model is stable and achieves an equilibrium state. For the model with a 24° joint, the top block slides along the inclined joint, as shown by the red velocity vectors of Figure 9. The velocity history confirms that the movement accelerates with time. Thus, the effective stress formulation of Slope Model and its predictions of the effect of fluid pressure on slope stability are in agreement with the analytic solution.

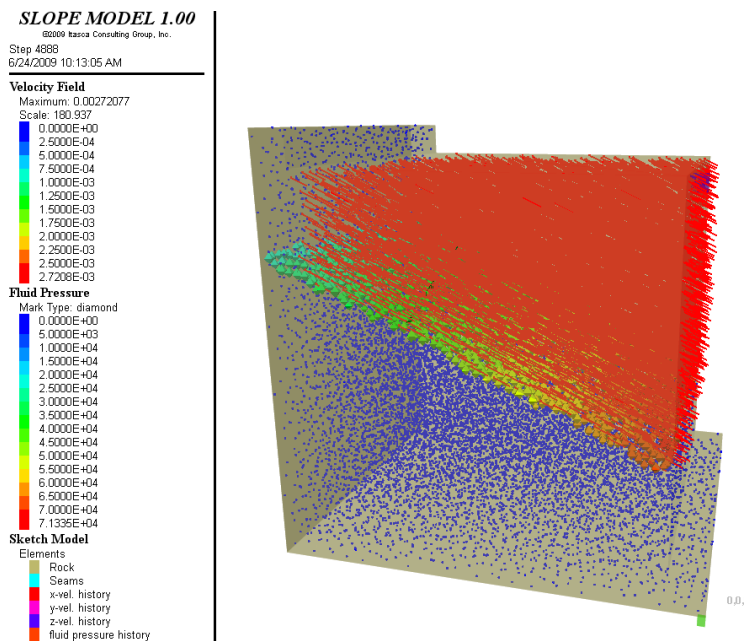


**Figure 9** – Velocity vectors shown for the case of 24o joint dip [Elevated velocities are shown in red. Fluid pressures are also shown as various colors within the joint plane. In this case, the upper block is unstable.]

### Fluid Pressure Response to Bench Excavation

The coupled hydro-mechanical formulation built into Slope Model allows the simulation of fluid pressure changes in response to rock mass deformation (e.g., excavation of benches). To demonstrate that capability, the simple system shown in Figure 10 is analyzed in Slope Model. A 30-m high slope has a horizontal, saturated joint. The fluid pressures in the joint on the west and east model boundaries are 2.5 MPa and 0.5 MPa, respectively. In the first stage of simulation, the model is run (with only the mechanical model active) until the gravitational in situ stress state is achieved. In the second stage, the bench indicated by the blue box is excavated. The model response to the bench excavation is simulated as fully coupled, with both mechanical and flow models active. The calculated pressure histories (versus time in seconds) at three points in the horizontal joint (i.e., three red squares in the joint plane shown in Figure 10) are shown in Figure 11. The histories show that the fluid pressure drops rapidly in response to mechanical deformation (i.e., dilation) of the joints after removal of the bench. After the mechanical model reaches equilibrium, the fluid pressures gradually recover as the flow model returns to steady state. The example demonstrates that Slope Model is able to simulate both the short-term and long-term fluid response to mechanical changes.

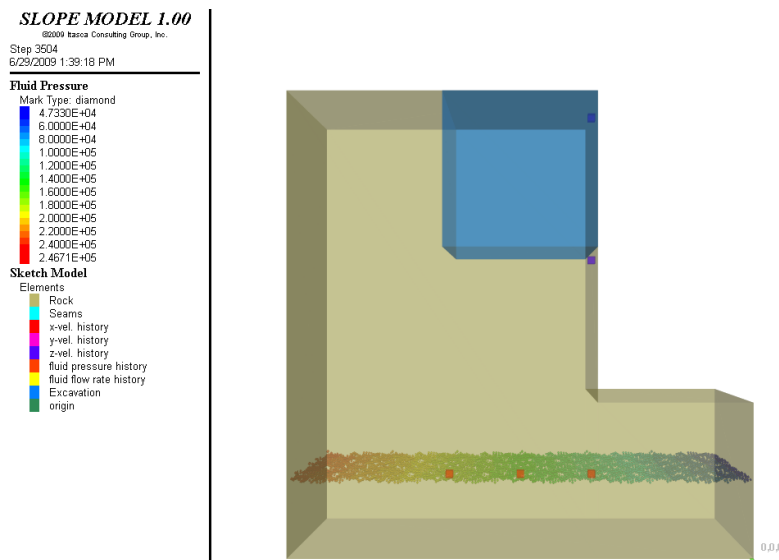


**Figure 10** – Initial geometry and fluid pressures for Slope Model simulation of pressure response to bench excavation [The blue box is the region to be excavated and the red icons are the locations of pressure monitoring points.]

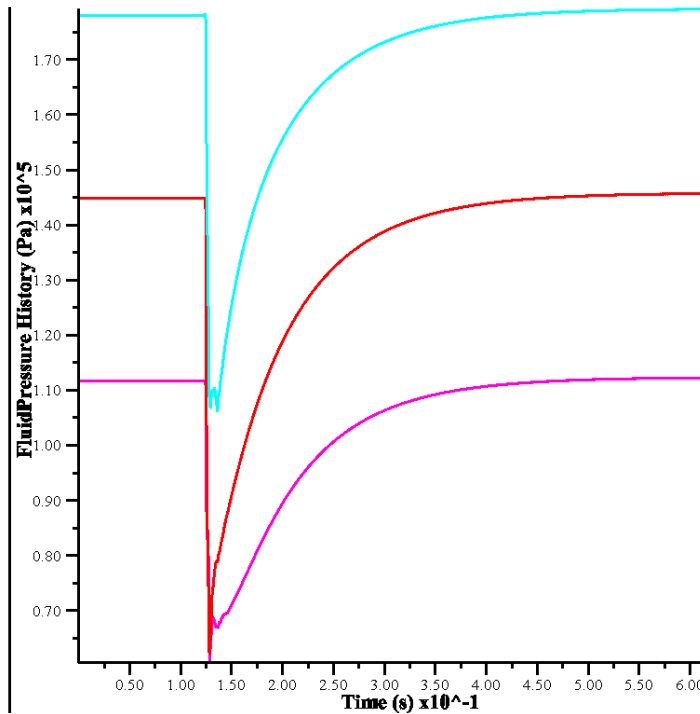


**Figure 11** – Fluid pressure response (versus time) at three locations following bench excavation [The rapid drawdown is due to the mechanical response (joint dilation), and the longer recovery is due to fluid flow acting to return the pressure field to steady state.]

## CONCLUSIONS

Slope Model is a powerful 3D simulator for jointed rock slopes that allows the main mechanisms (nonlinear mechanical response, fluid flow in joints and coupled fluid / mechanical interaction) to be reproduced. It is a true numerical model, unlike limit equilibrium methods or kinetic models, which do not embody the full physics. Slope Model is similar to 3DEC (5) with respect to the range of mechanisms that are reproduced, but Slope Model has the added capability to simulate the fracture of intact rock. The formulation of Slope Model is based on a quasi-random lattice of nodes and springs, rather than the elements or zones that are used by conventional modeling codes. Mesh-generation is automatic for any given slope geometry, and the resolution may be set with one user-controlled parameter. Thus, a coarse estimate of behavior may be made quickly, followed by a more accurate (but more time-consuming) simulation when difficulties have been resolved in the initial model. The code is quite new, and will need extensive testing before it should be used in support of design.

The lattice formulation of Slope Model is similar to that of the HSBM code BloUp (8), used for simulating the complete blasting process. In particular, the damage induced in a slope near the blast site can be quantified by BloUp, in terms of microcracks (broken lattice springs). It may be possible (in a future development) to import this damage field into Slope Model in order to include the effect of blast damage on slope stability.

## ACKNOWLEDGEMENTS

The work described here was performed under a Collaborative Research Agreement with the CSIRO in Brisbane, Australia as part of the Large Open Pit (LOP) Project. The Sponsors of this project are thanked for their support. Matt Purvance and Maurilio Torres of Itasca Consulting Group, Inc are thanked for their valuable coding work on Slope Model.

## APPENDIX: FORMULATION FOR SLOPE MODEL

### Mechanical Formulation

The lattice used in Slope Model is a quasi-random assembly of nodes connected by nonlinear springs. The mean distance between nodes is called the “resolution,” which may be set by the user to control the precision with which a given slope is modeled. All Itasca codes use an explicit solution scheme, which is well-suited to the direct simulation of highly nonlinear behavior such as fracture, slip and opening/closing of joints. The law of motion consists of the following central difference formulas for each node:

$$\begin{aligned} \dot{u}_i^{(t+\Delta t/2)} &= \dot{u}_i^{(t-\Delta t/2)} + \Sigma F_i^{(t)} \Delta t / m \\ u_i^{(t+\Delta t)} &= u_i^{(t)} + \dot{u}_i^{(t+\Delta t/2)} \Delta t \end{aligned} \tag{A.1}$$

where  $\dot{u}_i^{(t)}$  and  $u_i^{(t)}$  are the velocity and position (respectively) of vector component  $i$  ( $i = 1, 3$ ) at time  $t$ ,  $\Sigma F_i$  is the sum of all force-components  $i$  acting on the node of mass  $m$ , with the mechanical timestep  $\Delta t$ . Note that spins are assumed to be zero and that moments (arising from shear forces) do not act to cause rotations, which is equivalent to the assumption of infinite moments of inertia for nodes. These assumptions are made in the interest of code efficiency and are found to have only a minimal effect on the mechanical response of the system.

After all nodes have been visited (applying (A.1) to each one), a scan of all springs is performed. If a spring is unbroken, the following calculations are performed at time  $t$  (time superscript omitted for clarity).

$$\dot{u}_i^{\text{rel}} = \dot{u}_i^{\text{A}} - \dot{u}_i^{\text{B}} \quad (\text{A.2})$$

where the superscript “rel” denotes “relative”, and “A” and “B” denote the two particles connected by the spring.

$$\begin{aligned} \dot{u}^{\text{N}} &= \dot{u}_i^{\text{rel}} n_i \\ \dot{u}_i^{\text{S}} &= \dot{u}_i^{\text{rel}} - \dot{u}^{\text{N}} n_i \end{aligned} \quad (\text{A.3})$$

where “N” denotes “normal”, “S” denotes shear,  $n_i$  is the unit normal vector, and the Einstein summation convention applies to repeated indices. The normal and shear forces then are updated:

$$\begin{aligned} F^{\text{N}} &\leftarrow F^{\text{N}} + \dot{u}^{\text{N}} k^{\text{N}} \Delta t \\ F_i^{\text{S}} &\leftarrow F_i^{\text{S}} + \dot{u}_i^{\text{S}} k^{\text{S}} \Delta t \end{aligned} \quad (\text{A.4})$$

where  $k^{\text{N}}$  and  $k^{\text{S}}$  are the spring normal and shear stiffnesses, respectively, and the normal force is positive in tension. After calculation by (A.4), the normal force is tested for breakage: thus, if  $F^{\text{N}} > F^{\text{Nmax}}$ , then  $F^{\text{N}} = 0$ ,  $F_i^{\text{S}} = 0$ , and a “fracture flag” is set. During future calculations, the spring forces remain zero while the “gap” is positive, where gap,  $g$ , is calculated as follows.

$$g \leftarrow g + \dot{u}^{\text{N}} \Delta t \quad (\text{A.5})$$

As soon as the gap becomes zero, the spring calculation reverts to that of (A.4). Thereafter, the spring separates again ( $g > 0$ ,  $F^{\text{N}} = 0$ ) when the normal force becomes greater than zero. For a spring that is part of a joint segment, the shear force is limited to the maximum frictional force when the normal force is compressive ( $F^{\text{N}} < 0$ ):

$$\text{If } |F_i^{\text{S}}| > \mu |F^{\text{N}}| \text{ then } F_i^{\text{S}} \leftarrow \mu F_i^{\text{S}} \frac{|F^{\text{N}}|}{|F_i^{\text{S}}|} \quad (\text{A.6})$$

where  $\mu$  is the friction coefficient of the joint segment.

Finally, the new spring forces are added (with the appropriate signs) to the force-sums of the associated nodes:

$$\begin{aligned} \Sigma F_i^{\text{A}} &\leftarrow \Sigma F_i^{\text{A}} - (F^{\text{N}} - pA) n_i - F_i^{\text{S}} \\ \Sigma F_i^{\text{B}} &\leftarrow \Sigma F_i^{\text{B}} + (F^{\text{N}} - pA) n_i + F_i^{\text{S}} \end{aligned} \quad (\text{A.7})$$

For a regular spring (part of the intact rock material), the vector  $n_i$  is the unit normal from node A to node B — i.e.,  $n_i = (u_i^{\text{A}} - u_i^{\text{B}}) / |u_i^{\text{A}} - u_i^{\text{B}}|$ . Should a joint plane pass through the spring, then  $n_i$  is the unit normal to the joint plane rather than that of the associated spring. The terms  $pA$  in (A.7) account for the effect of fluid pressure  $p$  within the fluid element associated with the spring, where  $A$  is the apparent area of the fluid element.

## Fluid Formulation

Fluid flow takes place in the joints with non-zero aperture. The nodes (or elements) of the flow model are located at the lattice springs within the joints (i.e., the springs intersected by the joints). The flow nodes are connected by a random network of pipes. A flow node is connected to all nodes within a distance equal to the lattice resolution multiplied by the fluid resolution, which is a user-specified dimensionless parameter between 0.6 and 1.2 (with a default value of 0.8). The fluid pressure is a flow-node variable. The flow between nodes takes place along the pipes. It is assumed that the pipe width (in the joint plane) is equal to its length. The flow rate along a pipe, from flow node “A” to node “B”, is calculated based on the following relation:

$$q = \beta k_r \frac{a^3}{12\mu} [p^{\text{A}} - p^{\text{B}} + \rho_w g (z^{\text{A}} - z^{\text{B}})] \quad (\text{A.8})$$

where  $a$  is hydraulic aperture,  $\mu$  is viscosity of the fluid,  $p^{\text{A}}$  and  $p^{\text{B}}$  are fluid pressures at nodes “A” and “B”, respectively,  $z^{\text{A}}$  and  $z^{\text{B}}$  are elevations of nodes “A” and “B”, respectively, and  $\rho_w$  is fluid density. The relative permeability,  $k_r$ , is a function of saturation,  $s$ :

$$k_r = s^2 (3 - 2s) \quad (\text{A.9})$$

Clearly, when the pipe is saturated,  $s = 1$ , the relative permeability is 1. Dimensionless number  $\beta$  is a calibration parameter, a function of fluid resolution, used to match conductivity of a pipe network to the conductivity of a joint represented by parallel plates with aperture  $a$ . The calibrated relation between  $\beta$  and the fluid resolution is built into the code for discrete values of fluid resolution in a tabular form. The code linearly interpolates for  $\beta$  between the discrete table values. The evolution of the flow model with time is solved using an explicit numerical scheme. The pressure increment,  $\Delta p_{\text{fluid}}$ , during the flow timestep  $\Delta t_f$  is calculated as:

$$\Delta p_{\text{fluid}} = \frac{1}{V} \sum_i q_i K_w \Delta t_f \quad (\text{A.10})$$

where  $K_w$  is the fluid bulk modulus,  $V$  is the node volume, and the summation is over all flow rates,  $q_i$ , from the pipes connected to the node (positive sign in the case of inflow). For a coupled calculation, a further pressure increment is added during the mechanical timestep,  $\Delta t$ , as follows:

$$\Delta p_{\text{mech}} = \frac{\dot{u}^N}{a} K_w \Delta t \quad (\text{A.11})$$

After both timesteps, the pressure is updated as follows:  $p \leftarrow p + \Delta p_{\text{fluid}} + \Delta p_{\text{mech}}$ . The fluid pressure cannot be negative in this model. If fluid pressure drops to zero, further flow from the node or its expansion results in a decrease in saturation. (Saturation is always equal to 1 when the pressure is positive.) The change in saturation during timestep  $\Delta t_f$  while the fluid pressure is equal to zero is calculated from the following relation:

$$\Delta s = \frac{Q}{V} \Delta t_f \quad (\text{A.12})$$

During coupled simulations, the mechanical and flow modules are synchronized. The module with the smaller timestep is executed multiple times per timestep of the module with the longer timestep to keep both calculations in step.

Note that Slope Model also contains logic to bring a model to the initial steady states in both mechanical and fluid domains. In particular, a given in situ stress state may be specified. The in situ stress is understood to exist before the given slope is created.

## REFERENCES

1. M. Pierce, P. Cundall, D. Potyondy and D. Mas Ivars, "A Synthetic Rock Mass Model for Jointed Rock," Rock Mechanics: Meeting Society's Challenges and Demands (1st Canada-U.S. Rock Mechanics Symposium, Vancouver, Vol. 1: Fundamentals, New Technologies & New Ideas, E. Eberhardt et al., Eds. Taylor & Francis Group, London, 2007, 341-349.
2. D.O. Potyondy and P.A. Cundall, "A Bonded-Particle Model for Rock," International Journal of Rock Mechanics & Mineral Science, Vol. 41, No. 8, 2004, 1329-1364.
3. Itasca Consulting Group, Inc., PFC2D (Particle Flow Code in 2 Dimensions), Version 4.0, Minneapolis, Minnesota, 2008.
4. Itasca Consulting Group, Inc., PFC3D (Particle Flow Code in 3 Dimensions), Version 4.0, Minneapolis, Minnesota, 2008.
5. Itasca Consulting Group, Inc., 3DEC (3-Dimensional Distinct Element Code), Version 4.1, Minneapolis, Minnesota, 2007.
6. E. Hoek and J. Bray, Rock Slope Engineering. Institution of Mining and Metallurgy, London, 1974.
7. Itasca Consultants, SAS, 3FLO, Version 2.31, Ecully, France, 2006.
8. J.F. Furtney, P.A. Cundall and G.D. Chitombo, "Developments in Numerical Modeling of Blast Induced Rock Fragmentation: Updates from the HSBM Project," to be published in the Proceedings of FRAGBLAST 9, September 2009.